J. exp. Biol. (1977), 71, 187–203
With 11 *figures*
Printed in Great Britain

THE SWIMMING OF *NYMPHON GRACILE* (PYCNOGONIDA): THE VERTICAL LIFT FORCES GENERATED WHILE SWIMMING AT CONSTANT DEPTH

BY ELFED MORGAN AND STEPHEN V. HAYES

Department of Zoology and Comparative Physiology and Department of Mechanical Engineering, University of Birmingham

(*Received* 29 *April* 1977)

SUMMARY

1. The vertical lift forces generated by the legs of *Nymphon* while swimming at constant depth have been estimated graphically using drag constants determined by a sedimentation method. Drag both normal and tangential to the different segments of the leg has been considered.

2. When holding station *Nymphon* characteristically employs a low elevation beat in which the upward force produced during the power stroke of each leg only just exceeds the predominantly downward force generated during the recovery. An upward lift component is also produced late during the recovery stroke.

3. The legs beat in a vertical plane and an investigation of the moments at the joints of the leg suggests that much of the power stroke is gravity assisted.

4. The upward lift produced by all eight legs agreed fairly well on average with the sinking force due to the animal's weight in water, and the vertical lift fluctuates rhythmically throughout the leg beat cycle. The relationship between the swimming gait and the amplitude of these fluctuations has been investigated. During the gait most frequently used by the animal fluctuations in vertical lift were found to be minimal.

INTRODUCTION

Nymphon gracile is a delicate, long-legged pycnogonid which, although usually benthic, swims frequently both in laboratory aquaria (Morgan, Nelson-Smith & Knight-Jones, 1964) and in the sea (Fage, 1932). The unusual swimming pattern shown by this and by other related species has attracted the attention of a number of workers (Cole, 1901; Prell, 1910; Knight-Jones & Macfadyen, 1959; Morgan, 1971, 1972). With the exception of the second coxa the leg segments articulate sequentially in the vertical plane, and the legs beat dorso-ventrally in a metachronal sequence, starting from the rear so that the animal progresses dorsal side first.

The mechanics of the leg-beat cycle have been described in a previous communication, in which the relative drag force acting normal to the segments of the leg was calculated at different stages during the power stroke, assuming each segment to be a simple cylinder (Morgan, 1971). If the energy cost of swimming is to be investigated, however, as in the subsequent paper (Morgan, 1977), an estimate of the actual

drag is necessary for both power and recovery strokes, taking into account the spines and other irregularities on the surface of each segment. Moreover, where the propulsive segment is long relative to its thickness, the drag due to the component of velocity longitudinal to the segment must also be considered (Taylor, 1952). This is especially significant for *Nymphon* where, with the possible exception of the femur, the leg segments frequently move tangentially to their long axes. The range of Reynolds numbers involved between 1 and 10, is a difficult transitional one. At Reynolds numbers above 30 drag varies with the square of the velocity of the fluid moving over the segment, and depends on the density of the medium and the frontal area of the segment. For Reynolds numbers of less than 1, viscosity contributes more to the drag, which now varies directly with the velocity and the length of the segment (e.g. see Alexander, 1968).

In the present paper the relationship between drag and velocity has been investigated for different segments of the leg, using a sedimentation technique and the lift forces generated by leg beating have been calculated. The total instantaneous uplift will fluctuate as different legs contribute at different times during the leg-beat cycle. These variations in uplift could, if extensive, result in vertical movements of the body with an associated energy loss for the animal when holding station at constant depth. The relationship between uplift and swimming gait is thus of interest, and is also considered here.

METHODS

The drag forces acting on the legs during swimming were estimated from the results of sedimentation experiments. At terminal sinking velocity the opposing drag forced equalled a sinking force due to the weight of the specimen in water. Measurements were made on individual leg segments, and on complete legs of preserved specimens. Each joint or a complete leg was fully extended, and remained thus for the duration of the experiment. The extension was achieved by placing the legs in narrow glass capillary tubes before fixing the specimens. The relationship between drag and velocity was investigated in a series of experiments in which the sinking velocity was varied by inserting small weights (short lengths cut from suture wire of uniform diameter and known weight per unit length) into the legs or leg segments. Drag was produced normal to the longitudinal axis of the leg sample by inserting the weights midway along the length of the sample so that it sank horizontally through the water. Drag tangential to the longitudinal axis was produced by inserting the weights into one end of the sample. Specimens were washed in sea water to remove the fixative prior to an experiment, and experiments were carried out in sea water at 18 °C. Terminal sinking velocity was measured over a distance of 75 cm in a tall glass cylinder of oval cross-section and having a lesser diameter of 5 cm. Specimens were hoisted back between trials on a small tray of stainless-steel mesh. Measurements were made on a number of individuals but the data presented below is primarily for the legs of a single ovigerous male *Nymphon* with dimensions similar to those used previously in calculating the relative drag forces acting on the leg during the powerstroke (Morgan, 1971).

Using the above technique drag constants normal and tangential to the long axis of the segment were derived for the femur, tibia I, and the combined tibia II, tarsus and propodium segments. These constants have been used to calculate the lift forces

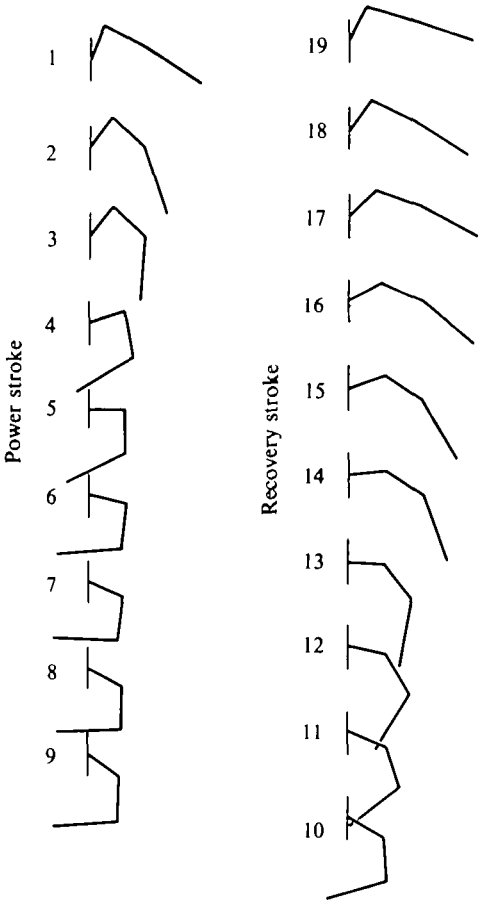

Fig. 1. Changes in profile of a single leg during a complete cycle of movement. The positions of individual segments were traced from consecutive frames of a ciné film taken at 18 frames/s. The three coxa segments are not shown and have not been considered in the analysis, and the tarsus and propodium are regarded as rigid extensions of tibia 2.

acting on the leg during swimming, using the method described in the Appendix. The actual coefficients of drag were not used in the calculation. The movements of the different segments were studied by analysis of ciné films taken at 18 or 24 frames/s, and the total lift forces generated by all eight legs was derived using the preferred gait described previously (Morgan, 1972). In this the contralateral legs of the same segment beat in antiphase, and ipsilateral legs 3 in 4, 2 in 4 and 1 in 2 with a phase delay of 0·3, 0·6 and 0·36 cycles respectively.

RESULTS

Experimental results

Articulation of leg segments

When swimming, the legs of *Nymphon* beat in a dorso-ventral plane, and follow a metachronal sequence, starting from the rear. The down stroke is the power stroke, and the animal moves through the water dorsal-side first. Swimming is normally

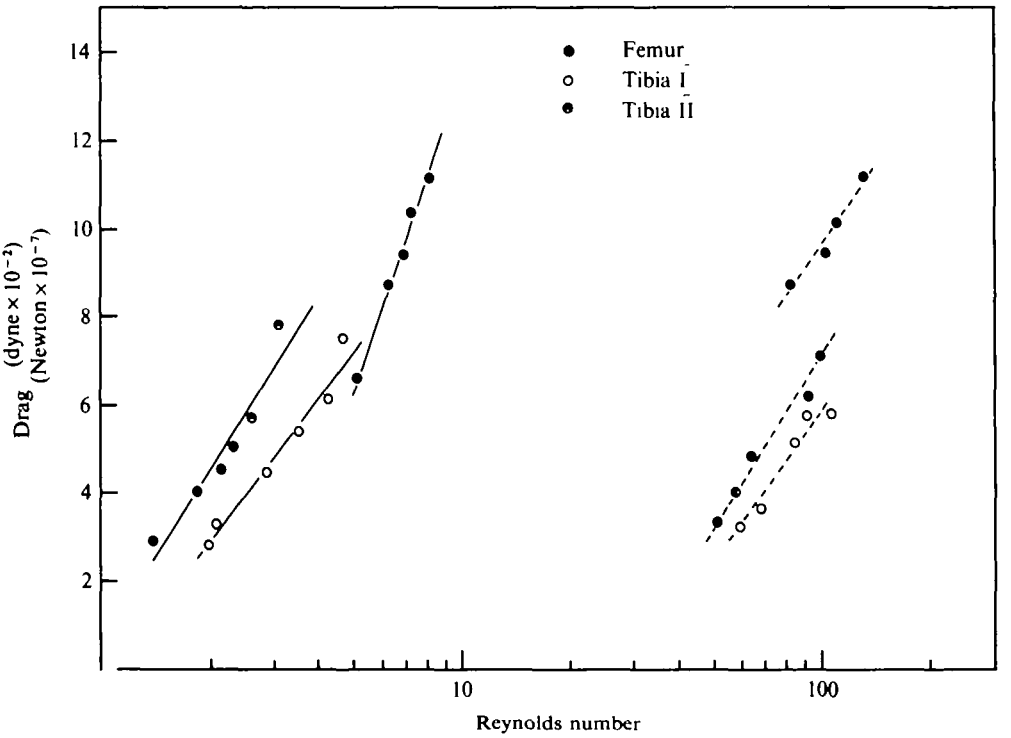

Fig. 2. The drag forces acting normal to (——) and tangential to (– – –) the long axes of the major segments of the leg, plotted against Reynolds number. The best fitting straight line has been drawn through the points in each case.

orientated towards the light source but in the diffuse lighting of the laboratory, specimens frequently hold station at constant depth, while orientated vertically in the water column. There is now no net movement of water relative to the body, and the drag forces acting on the legs result from their angular movements relative to the body (discounting possible interference between the legs).

The inclination of the femur to the vertical, and the angles between adjacent segments of the legs, were measured from single frames of a ciné film sequence of an animal swimming at constant depth. Fig. 1 shows the positions occupied by the major segments of the leg during a complete cycle of movement in which the femur moved through an arc of 105°, between 20° and 125° to the vertical. This is characteristic of an adult *Nymphon* when holding station, with a leg-beat frequency of about 1 c/s.

During the cycle of movement the joints of the leg articulate sequentially, so that the leg profile changes continuously throughout the beat, and different segments may often rotate in opposite directions. Thus during the power stroke, flexion of the tibial joint for example, results in tibia II, together with the tarsus and propodium, rotating inwards and upwards (frames 3–7) while the femur rotates downwards. Flexion of the femero-tibial joint at this time causes tibia I to articulate downwards, except for a brief period (frame 6) when the segment rotates beyond the vertically downward position. Conversely the subsequent extension of the joint brings about the upward rotation of tibia I later in the power stroke (see Fig. 1).

Fig. 3. Stereoscan electron micrograph showing spines and bifid setae on cuticle surface *Nymphon gracile* tibia 2.

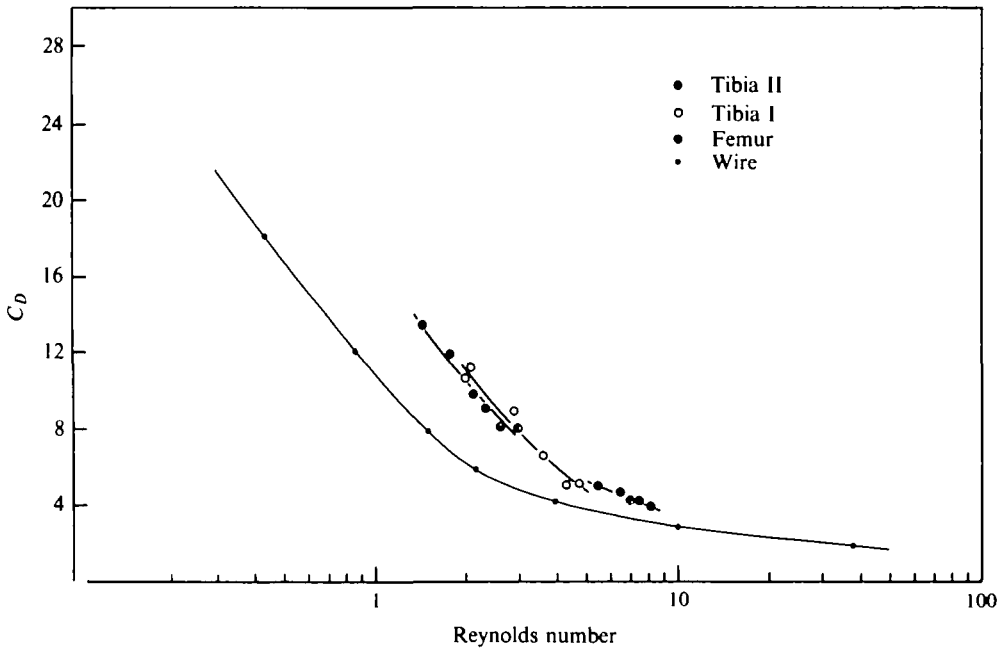

Fig. 4. The drag coefficients of each of the major segments of the leg, and the drag coefficients of a wire cylinder, plotted against Reynolds number.

Drag normal and longitudinal to the leg

A long cylindrical object, such as the leg of *Nymphon*, when moving through the water is subjected to drag forces acting both normal and longitudinal to its axis, and these forces will vary with the velocity. The relationship between velocity and drag has been investigated using the method described above, and Fig. 2 shows the relationship between drag and Reynolds number for the different segments sinking horizontally and vertically through the water. The range of velocities studied include those most frequently encountered during swimming. For a given velocity the tangential drag was found to be only about half that normal to the segment, and a similar relationship was found to exist between the normal and tangential drag forces acting over the whole leg. It is of interest to note therefore that an earlier record of sinking speeds (Morgan, 1971) shows the rate of passive descent for animals with the legs extended horizontally to be almost half that recorded when the legs are allowed to trail vertically in the 'plummeting' position. The relationship between drag and velocity was recorded for the individual segments of 14 different legs, and drag constants normal and tangential to the femur, tibia I and to the combined tibia II, tarsus and propodium were determined, assuming the latter two segments to be identical extensions of the second tibia.

Surface irregularities have little effect on drag unless they extend beyond the boundary layer (e.g. see Alexander, 1969). At Reynolds numbers of less than 10, however, the frictional component of drag increases in proportion and the roughness of the body surface now becomes of greater significance. In *Nymphon* immovable spines of up to 90 μm long, and numerous small bifid setae found on the surface of the cuticle (Fig. 3), may thus contribute to the drag. In Fig. 4 the drag coefficient of

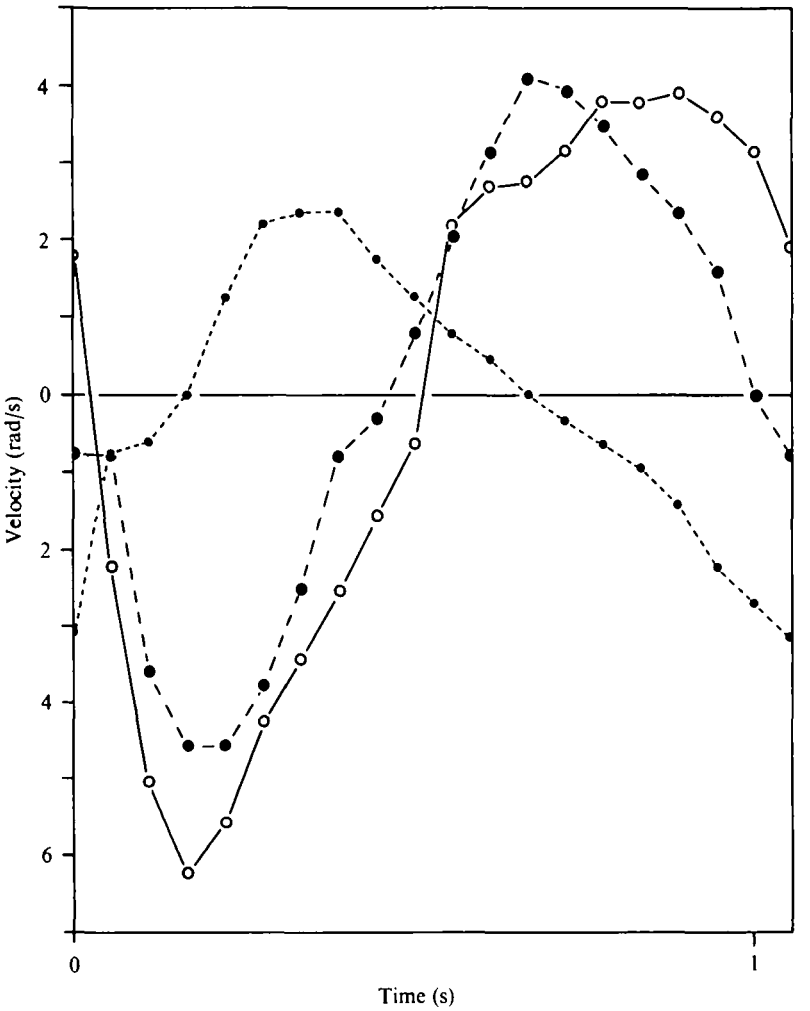

Fig. 5. The angular velocities of the femur (○), tibia 1 (●) and tibia 2 plus tarsus and propodium (◉) at different stages during the cycle of movement of a single leg. The values below the zero line indicate declination of the femur, and the flexion of the femero-tibial and tibial joints.

each segment when sinking horizontally is plotted against Reynolds number and may be compared with that of a smooth cylinder. The latter values were determined from measurements of the sinking velocity of short lengths of wire of known density in a commercial oil (Shell, Carnea 21). The different segments are not equally spinous, the femur being slightly less so than the two tibiae, but the difference does not appear to be a very significant one for at a Reynolds number of about 5 the drag coefficient of the femur is approximately equal to that of tibia I. Between Reynolds numbers of 1 and 10, however, the drag coefficients of the leg segments diverge significantly from those of a cylinder, becoming progressively greater with decreasing Reynolds number.

For the most part both spines and setae project towards the distal end of each segment and thus may conceivably contribute differentially to the drag during the

power and recovery strokes. However, experiments in which individual segments were weighted so as to sink with the distal, and then the proximal, end first revealed no significant difference between the sinking velocities at any given drag force.

Sinking force acting on the whole animal

When *Nymphon* holds station at constant depth the uplift generated by the swimming legs must balance the sinking force due to its own weight in sea water. The latter was measured directly by suspending the animal in sea water from one arm of a sensitive balance and, for the intact ovigerous male upon which the present study is based, was found to be 1·34 dyne, to which the egg masses on the ovigers contributed a sinking force of 0·35 dyne.

Calculated results

Angular velocities of different leg segments

The angular velocities of the femur, tibia I and the combined tibia II, tarsus and propodium have been calculated at different stages during the beat of a single leg, and are shown in Fig. 5. The angular velocity of each segment follows an approximately sinusoidal wave form, with the femoro-tibial joint starting to open out about one third of the way through the down stroke (= power stroke) of the femur. The angle between tibia I and tibia II remains fixed at the beginning of the power stroke, and the angular movement of tibia II on tibia I thus follows the rotation of the femur with a slight phase delay, flexion of the joint occurring mainly during the power stroke. Extension of the femoro-tibial joint may be facilitated to some extent by the downward rotation of the femur and the resistance of the water to the tibia I segment. Maximum extension velocity of tibia I does not coincide with the maximum angular velocity of the femur during the power stroke, however, but occurs about 160 ms later.

Lift forces generated by a single leg

The rotation of the leg about its coxal pivots results in drag forces acting normal to, and parallel to, each segment of the leg, and each may be resolved into its vertical and lateral components. Only the vertical forces are used in maintaining constant depth, and the lateral drag components have not been considered here. The slight vertical movements of the body while holding station were disregarded in the initial calculation and hence the rotation of the femur was considered not to generate a drag force tangential to its own longitudinal axis. The drag forces acting on each segment of the leg were calculated according to the equations given in the Appendix, and the vertical components of lift derived. Fig. 6 shows the vertical lift derived from drag normal to, and longitudinal to, the different segments of the leg over the complete cycle of movements described above.

During the power stroke the femur reaches maximum angular velocity when it is inclined almost horizontally, and hence greatest uplift is generated at this time. During the recovery maximum downward lift again occurs at approximately maximum velocity, but the femur is now more vertically inclined, and the magnitude of the force is less than that generated during the power stroke. Tibia I is almost vertical for much of the power stroke, so that most of the uplift is derived from drag along the long axis of the segment (see Fig. 1). Horizontal movements are slight, and drag normal to tibia I contributes negligible vertical lift at this time.

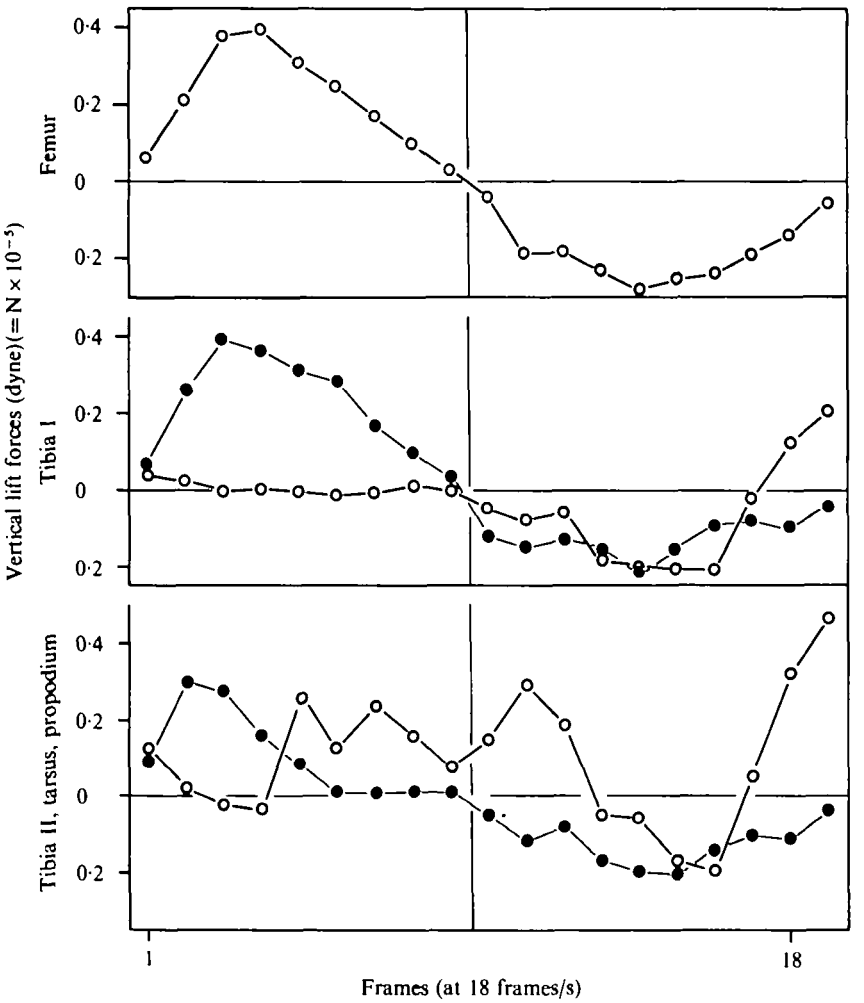

Fig. 6. The vertical lift forces generated by the three major segments of the leg, derived from drag acting normal to (○) and tangential to (●) their long axes. Values below zero indicate a downward lift in each case.

The lift forces summated over the entire leg at different stages in the leg beat cycle are shown in Fig. 7, together with the components due to drag normal and tangential to the segments. Tangential drag contributes about half the total vertical lift force, but the instantaneous lift owing to drag normal to the leg segments shows greater fluctuation over the leg beat cycle. This component generates two periods of uplift during the beat, with maxima midway through the power stroke, and towards the end of the recovery.

When the sum of normal and tangential lift components is considered, the upward lift generated during the power stroke exceeds the downward lift produced during the recovery, as is to be expected, and the average vertical lift calculated over this particular cycle was found to be an upward force of 0·15 dyne (15 μN).

The swimming legs beat in a vertical plane and, despite their small mass, gravity will therefore promote or oppose the rotation of the individual segments at different

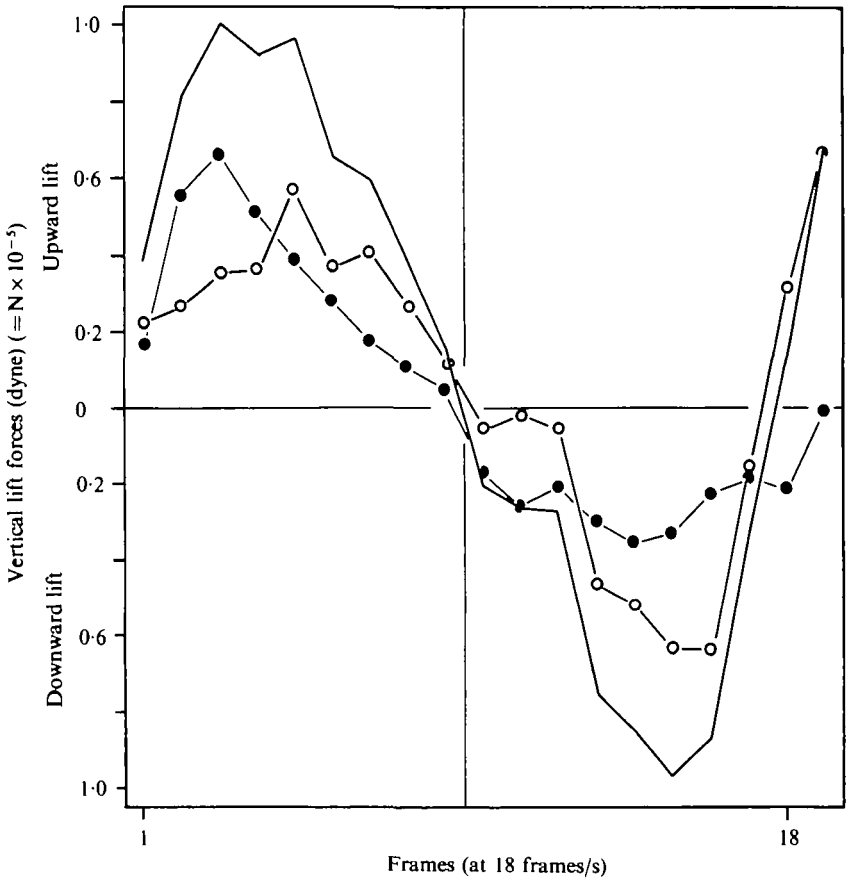

Fig. 7. The summated vertical lift forces due to normal (○) and tangential (●) drag are shown during a single beat, together with the total vertical lift produced by the entire leg.

stages during the leg beat. The extent of this gravitational influence has been investigated by calculating the moments about the proximal joints of the femur and of the first and second tibia segments, using the method in the Appendix. In Fig. 8 the moments due to gravity acting on these segments are compared with the moments of the drag forces opposing angular rotation about the proximal pivots of the segments. The rotation of the femur during the power stroke is a downward one and the gravitation of moments due to the weight in water of the whole leg about the proximal joint of the femur are also downward at this stage. During the early part of the power stroke the moments expected if the leg was rotating under the influence of gravity alone are on average about half those of the opposing drag force, and towards the end of the power stroke they actually exceed the latter indicating that the limb is allowed to fall under its own weight at this stage. During the recovery stroke on the other hand both the gravitational and the drag forces opposing the movements of the leg are coincident. The gravitational moments of the first and second tibia segments, tarsus and propodium about the femoro-tibial joint will also assist in the flexion of the joint during the power stroke except for a brief instant when tibia I rotates beyond the vertically downwards position (see frames 6 and 7, Fig. 1). The extension of tibia II

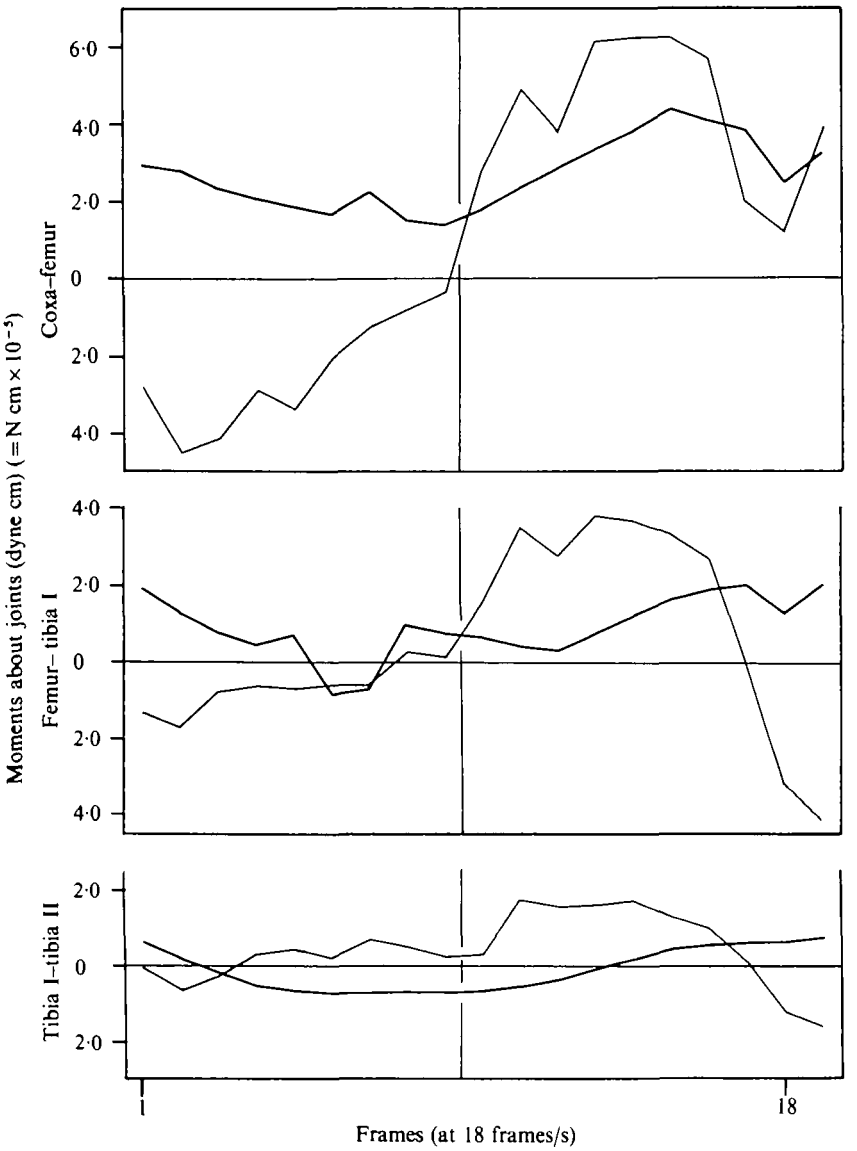

Fig. 8. The moments produced at the proximal joints of the femur, tibia 1 and tibia 2 by gravitational (——) and viscous drag (——) forces acting on the different segments. Gravity exerts a constant downward force throughout, but will support or oppose the movement of the leg segment depending upon the inclination of the segment to the vertical.

is similarly gravity-assisted for the most part, and the initial extension of this segment (see frames 8, 9 and 10, Fig. 1) could well be a passive process.

Lift forces generated by all eight legs.

Assuming the lift forces to be the same on average for all eight legs, then during the most commonly used swimming gait (Morgan, 1972) each leg would contribute to the total lift in a metachronal sequence, as shown in Fig. 9. The total lift is now always upwardly directed and the total uplift averaged by all eight legs over a complete

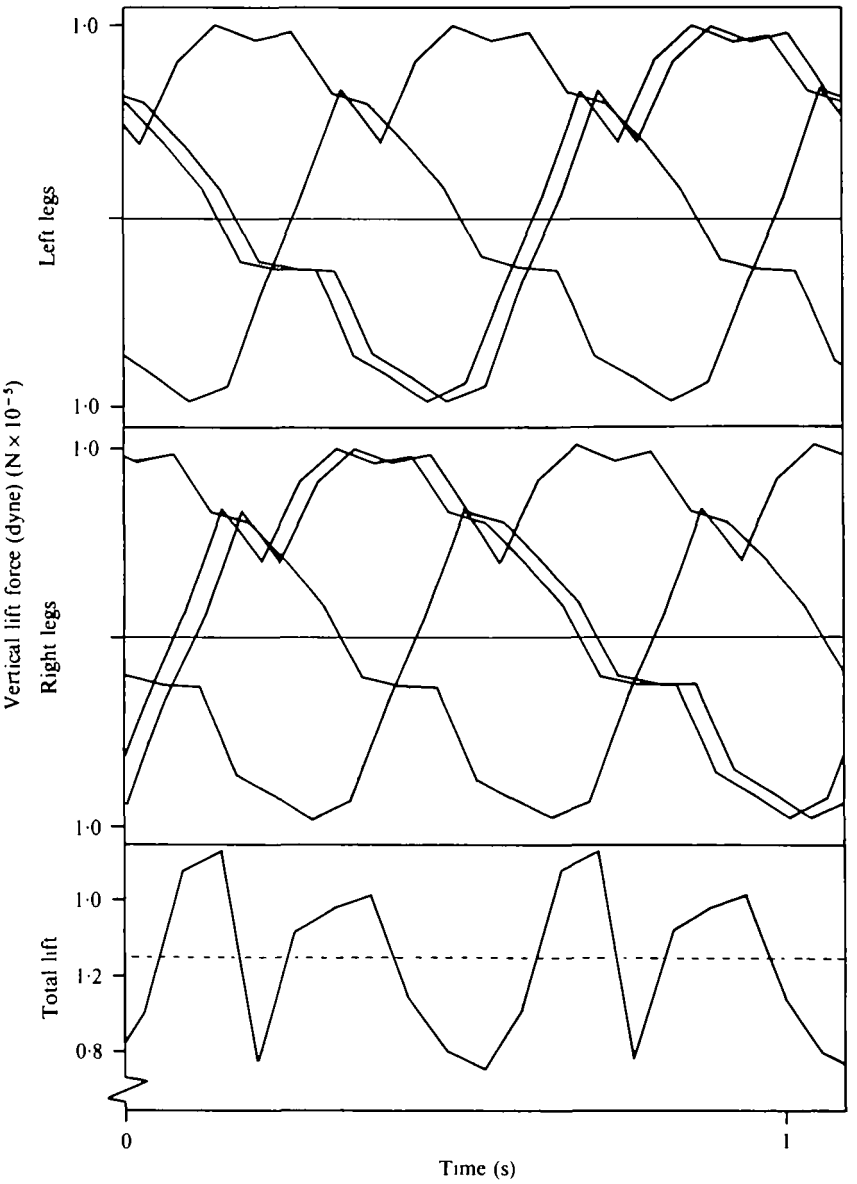

Fig. 9. The vertical lift forces generated by all eight legs during a complete leg-beat cycle while swimming at constant depth.

leg-beat cycle was found to be 1·20 dyne (12 μN). This approximates closely to the sinking force of 1·34 dyne (13·4 μN) due to the weight of the animal and ovigers in sea water. The uplift fluctuates rhythmically between about 0·6 and 1·8 dyne (6–18 μN) with four periods of near maximum lift occurring within a single leg-beat cycle, and periodic fluctuations of this sort would be expected to cause the animal to move up and down in the water. These vertical oscillations have been disregarded in the above calculations and thus represent a potential source of error. Moreover, such movements

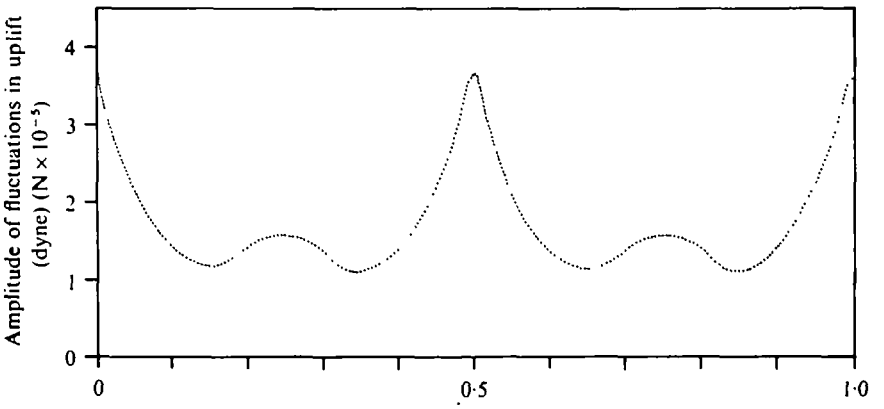

Fig. 10. The amplitude of fluctuations in upward lift produced by all eight legs expected at different phase delays, assuming the same delay between each ipsilateral leg, and the contrololateral legs to beat in antiphase.

could be energy-consuming, and if extensive could impair the animal's swimming efficiency. However, as both mass and upward force are known the acceleration may be calculated, and hence so may the velocity and vertical displacement of the animal at different times during the beat. Assuming *Nymphon* to sink under its own weight when the summated uplift is less than the sinking force the maximum amplitude of vertical movements which could be produced by the forces shown in Fig. 9 would be $8{\cdot}7 \times 10^{-2}$ cm and the maximum velocity of such movements about 0·52 cm/s.

Relationship between uplift and swimming gait

As may be seen from Fig. 9, the upward impulse produced by each of the legs fluctuates rhythmically during the leg-beat cycle, and the amplitude and frequency of these oscillations during a complete leg beat cycle will depend on the sequence of movements of the different legs.

Using the lift values calculated previously for the entire leg (Fig. 6) the relationship between amplitude and swimming gait was investigated in a model in which the same phase delay was assumed between each adjacent ipsilateral leg. These were assumed to beat in metachronal sequence, starting from the rear, and the contralateral legs were assumed to beat in antiphase. The drag on the body is small, less than 0·02 dyne (0·2 μN), at velocities of below 0·5 cm/s. (Morgan, unpublished data) and was disregarded. Also, as the mass of each limb is small (less than 3 % of that of the body plus ovigers), the inertial effects due to the acceleration of the legs have not been taken into consideration. The amplitude of oscillations in uplift during the course of a single leg-beat cycle, predicted for phase delays from 0 to 1 between adjacent ipsilateral legs, is shown in Fig. 10.

Greatest fluctuations in uplift are to be expected when all four ipsilateral legs beat exactly in phase (i.e. with a phase lag of 0 or 1), and at a phase delay of 0·5 cycle when alternate ipsilateral and controlateral legs beat together, but these gaits are probably rarely, if ever, employed by the intact animal. Minimum fluctuations in uplift, on the other hand, will occur at phase delays of 0·15, 0·35, 0·65 and 0·85 cycle respectively, and it is significant that the phase values most frequently used by *Nymphon* when swimming are approximately 0·3–0·35.

DISCUSSION

Swimming at constant depth presents a problem to *Nymphon*, for the swimming legs beat in a dorso-ventral plane and the main propulsive force is directed vertically, upwards. Unlike the hairs on the legs of *Dytiscus* (Hughes, 1958) the spines and setae on the different segments of the leg of *Nymphon* provide little or no control over the propulsive force generated during the swimming stroke. The spines are fixed and the setae probably trail passively in the water current. Over the range of velocities most frequently encountered during swimming these projections do not contribute differentially to the drag during the power and recovery strokes, and it seems likely that the setae are sensory as King (1973) has suggested. One way in which the animal is able to regulate the lift it produces is by lowering the elevation of the arc of movement of the femur. The leg-beat cycle described above is characteristic of an ovigerous male *Nymphon* when holding station and the pattern of movement of individual segments of the leg is such that the amplitude of the fluctuations in lift produced by the entire leg during the power and recovery strokes is kept to a minimum. Most of the upward lift produced during the power stroke of each leg is used to overcome the downward force generated during its recovery, and the mean uplift per beat is low compared with the average vertical lift produced during the power and recovery strokes independently. Analysis of moments about the joints of the leg indicates that much of the power stroke is gravity-assisted, although the kinetic energy so released is regenerated during the recovery phase of the beat and it is signficant to note that the fan-shaped elevator muscles which originate in coxae 2 and 3 appear to be considerably more powerful than those responsible for the declination of the femur. Because of the sequential articulation of the distal joints of the leg, and the low elevation of the arc of movement of the femur, the limb generates less lift than it might otherwise do during the power stroke (cf. Morgan, 1971) but upward lift is also produced during part of the recovery. The more extreme fluctuations between upward and downward lift which would occur during a higher elevation beat are thus avoided, and any vertical movements of the body which might result from these are therefore reduced.

On average there is fairly good agreement between the total vertical lift force generated by all eight legs, calculated for an animal holding station at constant depth, and that required to keep it from sinking through the water. The calculated mean total uplift falls short of the animal's weight in water by only 0·14 dyne (1·4 μN), approximately 10%. This discrepancy is within the margin of error to be expected where so many assumptions have been made. For example, the tarsus and propodium, regarded her as rigid extensions of the second tibia, have no extensor muscles and trail passively during the recovery stroke (Prell, 1910; Morgan, 1971). The drag along the length of these segments during this time will therefore be slightly greater than the calculated values.

Within the range of velocities studied the drag coefficient of each segment is higher than that of a smooth cylinder, indicating that the surface irregularities contribute significantly to the overall drag. This contribution will be especially important at low Reynolds numbers as the frictional component of drag increases, and at Reynolds numbers of less than 1 drag varies with length rather than with the area of the body (e.g. Alexander, 1968). It is conceivable therefore that the forces generated at the very beginning and end of the stroke, when the angular velocities are low, could be rather

higher than the calculated values. The total upward force fluctuates rhythmically throughout the leg-beat cycle, with a difference of just over 1 dyne between the maximum and minimum uplift generated by all eight legs, and the swimming gait employed by *Nymphon* appears to be optimal for producing a relatively constant, uniform upthrust. In practice the phase delay between adjacent ipsilateral legs is rarely exactly the same for each leg pair and the amplitude of oscillations in vertical lift calculated for the most frequently used gait was actually slightly lower than the lowest values predicted by the model (Fig. 10). These variations in lift would be expected to produce only slight vertical movements of the body in the water, and the energy lost in this way presumably would be small.

While the sequence of swimming leg movements may influence the variations in total vertical lift, the limits of this force will be determined by the movements of individual legs. With a low elevation beat approximately equal vertical forces are produced during power and recovery strokes, and it is debatable therefore whether holding station is very economical in its energy requirements. An estimation of the energy cost is given in the subsequent paper (Morgan, 1977).

REFERENCES

ALEXANDER, R. M. (1968). *Animal Mechanics*. London: Sidgwick and Jackson.

COLE, L. J. (1901). Notes on the habits of Pycnogonids. *Biol. Bull, mar. biol. Lab., Woods Hole* **2**, 195–207.

FAGE, L. (1932). Pêches planctoniques à la lumière effectuées à Banyuls sur Mer et à Concarneau. II. Pycnogonides. *Archs Zool. exp. gén.* **76**, 105–248.

HUGHES, G. M. (1958). The co-ordination of insect movements. III. Swimming in *Dytiscus*, *Hydrophilus*, and a dragonfly nymph. *J. exp. Biol.* **35**, 567–583.

KING, P. E. (1973). *Pycnogonids*. London: Hutchinson.

KNIGHT-JONES, E. W. & MACFADYEN, A. (1959). The metachronism of limb and body movements in annelids and arthropods. *Proc. XVth Int. Congr. Zool.* 969–971.

MORGAN, E., NELSON-SMITH, A. & KNIGHT-JONES, E. W. (1964). Responses of *Nymphon gracile* (Pycnogonida) to pressure cycles of tidal frequency. *J. exp. Biol.* **41**, 825–836.

MORGAN, E. (1971). The swimming of *Nymphon gracile* (Pycnogonida). The mechanics of the leg-beat cycle. *J. exp. Biol.* **55**, 273–287.

MORGAN, E. (1972). The swimming of *Nymphon gracile* (Pycnogonida). The swimming gait. *J. exp. Biol.* **56**, 421–432.

MORGAN, E. (1977). The swimming of *Nymphon gracile* (Pycnogonida). The energetics of swimming at constant depth. *J. exp. Biol.* **71**, 205–211.

PRELL, H. (1910). Beiträge zur Kenntniss des Lebensweise einiger Pantopoden. *Bergens Mus. Aarbog.* **10**, 30 pp.

TAYLOR, G. (1952). Analysis of the swimming of long and narrow animals. *Proc. R. Soc. Lond.* **214**, 158–183.

APPENDIX

Calculation of the drag forces acting on the leg segments of Nymphon gracile

In a previous study of swimming-leg mechanics relative drag forces were calculated for unit lengths of each leg segment, assuming each to be a simple cylinder (Morgan, 1971). Only the drag forces acting normal to the segments were considered and spines or irregularities on the surface of the segments were disregarded. If an estimate of absolute drag is required, however, these must be considered, together with the drag forces acting along the length of the cylinder.

The drag forces acting on a cylindrical body, *AB*, moving with rotation and translation in plane motion through the water will be dependent on the

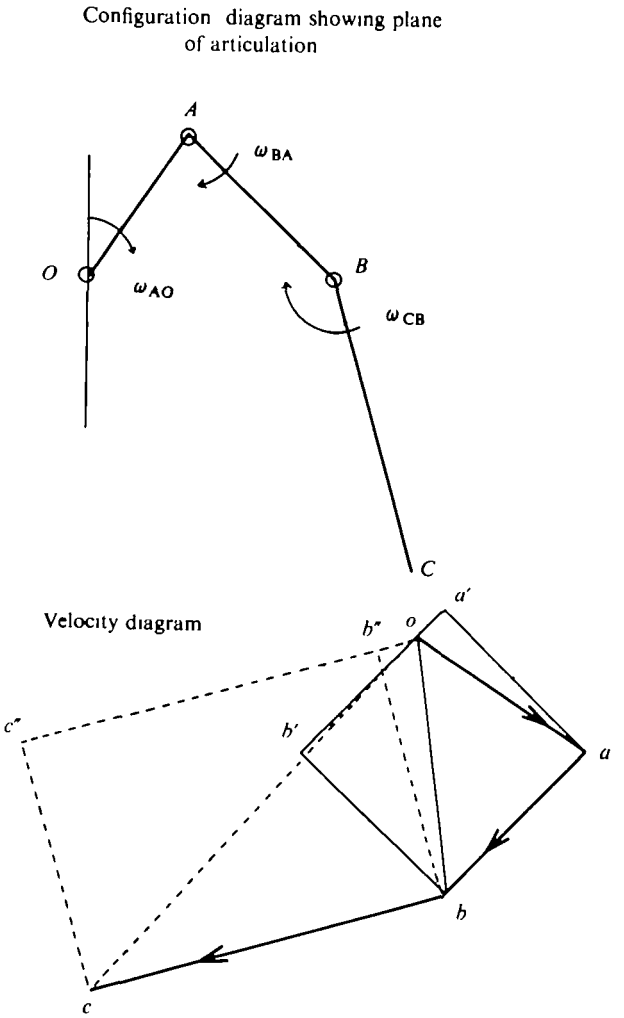

Fig. 11. Configuration diagram and velocity diagram used to determine the velocities at the extremities of the different segments. *OA*, *AB* and *BC* represent the femur, tibia 1, and tibia 2 plus tarsus and propodium, respectively; *oa*, *ab* and *bc* are the velocities at right angles to these segments resulting from the angular velocities ωAO, ωBA and ωBC respectively, and *oa*, *ob* and *oc* are the velocity vectors at *A*, *B*, and *C*. The velocities normal to *AB* at *A* and at *B* are given by *oa'* and *ob'*, and those normal to BC at *B* and *C* are given by *ob''* and *oc''*. The lengths *aa'* (= *bb'*) and *bb''* (= *cc''*) are the velocities of longitudinal movement along *AB* and *BC*.

velocity of movement, and if V'_A and V'_B are the velocities at the extremities then the velocity of any point x along its length is given by

$$V = V'_A + \omega x, \tag{1}$$

where ω is the angular velocity in radians. Similarly,

$$V'_B = V'_A + \omega L, \tag{2}$$

where L is the length of the body and

$$\omega L = V'_B - V'_A. \tag{3}$$

In the present analysis the slight vertical movements in the water which could result from variation in the summated up-thrust of the swimming legs have been ignored. The femur may thus be regarded as moving only perpendicularly to its long axis whereas tibia I, and also tibia II together with the tarsus and propodium are subjected to additional velocities resulting from the articulation of the femur and of the femur and tibia I respectively. The angular velocity of each segment about its proximal pivot was therefore determined separately from ciné film analysis and the velocity values calculated vectorally as in Fig. 11. Occasionally, due to the pattern of articulation of the leg, the velocities at the ends of individual segments were of opposite sign. In this situation equations (1)–(3) above now take the form:

$$V = -V'_A + \omega x,$$
$$V'_B = -V'_A + \omega L \quad (\omega L = V'_A + V'_B).$$

The drag force (F_T) acting normal to the long axis of the segment may now be calculated:

$$F_T = \int_0^L K_L . V . dx,$$

where K_L is a drag constant per unit length per unit velocity.

From equations (1), (2) and (3) above:

$$\begin{aligned} F_T &= K_L \int_0^L (V'_A + \omega x)\, dx = \frac{K_L}{2\omega}\left\{\left[V'_A + \omega x\right]^2\right\}_0^L \\ &= \frac{K_L}{2\omega}\left[V'^2_B - V'^2_A\right] = \frac{K_L}{2\omega}(V'_B + V'_A)(V'_B - V'_A) \\ &= K_L . L . \left(\frac{V'_B + V'_A}{2}\right) \\ &= K_L . L . V_{\text{mean}}. \end{aligned} \tag{4}$$

The drag force (F_A) due to the component of velocity acting along the length of the segment is similarly given by

$$K_A . L . V_{\text{axial}}$$

and the drag constants K_L and K_A were calculated from the above expressions after recording the settlement rates of weighted individual segments (see Methods).

The moment (M_A) of the transverse drag force may be calculated:

$$\begin{aligned} M_A &= \int_0^L K_L . V_x . x . dx. = K_L \int_0^L (V'_A + \omega x) x . dx. \\ &= K_L[V'_A . \tfrac{1}{2}x^2 + \omega \tfrac{1}{3}x^3]_0^L = K_L[V'_A + \tfrac{2}{3}\omega L]\tfrac{1}{2}L^2 \\ &= K_L[V'_A + \tfrac{2}{3}(V'_B - V'_A)]\tfrac{1}{2}L^2 \\ &= K_L[\tfrac{1}{3}V'_A + \tfrac{2}{3}V'_B]\tfrac{1}{2}L^2. \end{aligned} \tag{5}$$

The centre of moment $\bar{x}$, is now given by

$$\begin{aligned} \bar{x} &= \frac{\sum_0^L K_L . V . x . dx}{\sum_0^L K_L . V . dx.} = \frac{K_L[\tfrac{1}{3}V'_A + \tfrac{2}{3}V'_B]\tfrac{1}{2}L^2}{K_L[V'_B + V'_A]\tfrac{1}{2}L} \\ &= \left(\frac{\tfrac{1}{3}V'_A + \tfrac{2}{3}V'_B}{V'_A + V'_B}\right)L. \end{aligned} \tag{6}$$

When velocities of different sign at opposite ends of the same segment gave rise to a couple about a point of zero velocity the forces generated by each half segment, and their centres of moment were calculated separately before being summated for the whole segment, but when calculating the moments due to gravity the centre of mass of each segment was considered to be a a point half-way along its length.